PROCEEDINGS OF SCIENCE

Studies of unconventional baryon structure in the light quark sector with the BGOOD photoproduction experiment

T. C. Jude,[a,*] D. D Burdeinyi,[b] A. J. Clara Figueiredo,[a] R. Di Salvo,[c] A. Fantini,[c,d] O. Freyermuth,[a] F. Frommberger,[a] V. B Ganenko,[b] J. Groß,[a] K. Kohl,[a] P. Levi Sandri,[e] M. Ludwig,[a] L. Lutter,[a] P. Pedroni,[f] M. Romaniuk,[g] H. Schmieden[a] and A. Sonnenschein[a]

[a] *Physikalisches Institut, Universität Bonn, Germany*
[b] *Kharkov Institute of Physics and Technology, Ukraine*
[c] *INFN Roma "Tor Vergata", Rome, Italy*
[d] *Università di Roma "Tor Vergata", Dipartimento di Fisica, Rome, Italy*
[e] *INFN - Laboratori Nazionali di Frascati, Italy*
[f] *INFN sezione di Pavia, Italy*
[g] *Institute for Nuclear Research of NASU, Kyiv, Ukraine*

E-mail: jude@physik.uni-bonn.de

The discoveries of the pentaquark states and XYZ mesons in the charmed quark sector initiated a new epoch in hadron physics, where the existence of exotic multi-quark states beyond the conventional valence three quark and quark-antiquark systems has been confirmed. Such states could manifest as single colour bound objects, or evolve from meson-baryon and meson-meson interactions, creating molecular like systems and re-scattering effects near production thresholds. Equivalent structures may be evidenced in the light, uds sector, which is the focus of research at the BGOOD photoproduction experiment located at the ELSA accelerator at the University of Bonn (Germany). BGOOD is comprised of a central electromagnetic calorimeter and forward spectrometer, enabling access to low momentum exchange kinematics. This is crucial to study spatially extended, molecular-like structure which may manifest in reaction mechanisms.

Our results in the strangeness sector suggest a dominant role of meson-baryon dynamics which has an equivalence to the P_C states in the charmed sector. This includes structure in $K^0\Sigma^0$ and $K^+(\Lambda(1405) \to \pi^0\Sigma^0)$ photoproduction at the K^*Y threshold and a peak at the K^+K^-p threshold in $K^+\Sigma^-$ photoproduction which is only evident at very low momentum transfer kinematics.

In the non-strange sector, our measurements of the coherent reactions, $\gamma d \to \pi^0\pi^0 d$, $\gamma d \to \pi^0\eta d$ and $\gamma d \to \pi^0\pi^0\pi^0 d$ exhibit forward differential cross sections an order of magnitude higher than phenomenological model calculations. This is consistent with intermediate dibaryon formation, including the proposed $d^*(2380)$ hexaquark, however other mechanisms, such as final state interactions may yet prove to play dominant roles.

The 21st International Conference on Hadron Spectroscopy and Structure (HADRON2025)
27 - 31 March, 2025
Osaka University, Japan

*Speaker

ISSN 1824-8039. Published by SISSA Medialab.

PoS(HADRON2025)183

1. Introduction

Exotic, multi-quark states beyond valence three-quark and quark-antiquark systems are now unambiguously realised in the heavy, charmed quark sector. Many of these states, such as the P_c pentaquarks [1, 2] and XYZ mesons reside close to open charm thresholds, indicative of molecular-like structure. Equivalent structures may also be evidenced in the light, *uds* sector, including the $\Lambda(1405)$ and a cusp-like structure in $K^0\Sigma^+$ photoproduction at the $K^*\Sigma$ threshold [3, 4]

Experimentally, access to a low momentum exchange regions in reaction mechanisms is mandatory to elucidate the role of molecular-like structure if they are loosely bound and spatially extended systems. In a photoproduction experiment with a fixed target, this corresponds to forward meson acceptance to ensure the recoiling hadron system has minimal momentum transfer. The BGOOD experiment [5] (Fig. 1) at the ELSA electron accelerator facility [6, 7] is ideally suited for this. A 3 GeV electron beam impinges upon a thin radiator to produce an energy tagged bremsstrahlung photon beam which is subsequently incident upon a liquid hydrogen or deuterium target. BGOOD is comprised of two main parts, a central calorimeter region ideal for the reconstruction of neutral mesons via their decays (Fig. 2), and a forward spectrometer used for charged particle identification and momentum reconstruction at forward angles (Fig. 3).

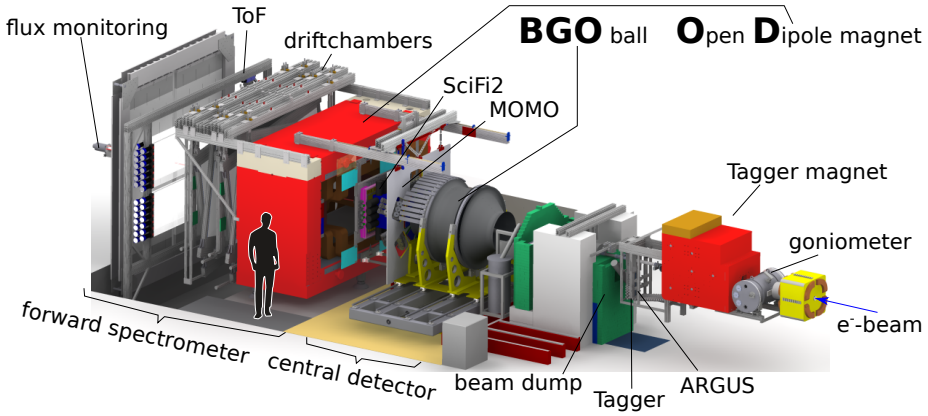

Figure 1: Schematic of the BGOOD photoproduction experiment. Figure from Ref. [5].

2. Strangeness photoproduction at BGOOD

BGOOD has an extensive strangeness photoproduction physics programme [8–14] with an emphasise on studying reactions at low momentum transfer (low t). This is achievable via the identification of K^+ in the forward spectrometer.

2.1 K^+Y photoproduction at forward angles and low momentum transfer

Fig. 4 shows differential cross section measurements at $\cos\theta^K_{\mathrm{CM}} > 0.9$ for $K^+\Lambda$ [10] and $K^+\Lambda(1520)$ [12] (left and right respectively). These are the first statistically precise measurements from threshold at the most forward $\cos\theta^K_{\mathrm{CM}}$ interval.

The $K^+\Sigma^0$ differential cross section for $\cos\theta^K_{\mathrm{CM}} > 0.9$ [11] (Fig. 5, left panel) exhibits a cusp-like structure close to the pK^+K^- threshold at $W \sim 1900$ MeV. This becomes most pronounced at

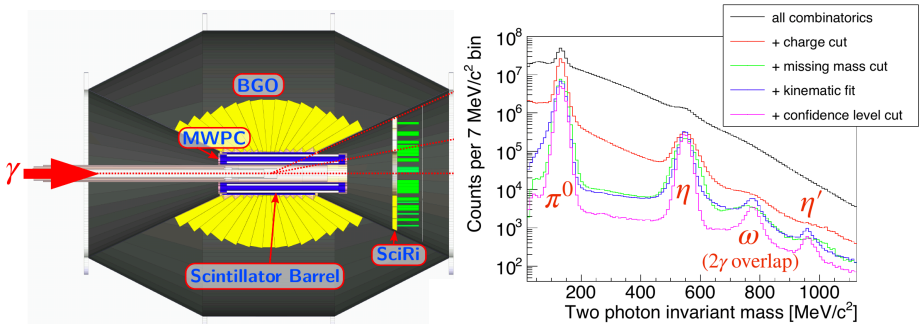

Figure 2: Left: A slice view of the central detector (photon beam entering from the left) consisting of the segmented BGO Rugby Ball, cylindrical inner Scintillator Barrel, MWPC, and the SciRi scintillator ring detector covering the intermediate region. Right: The invariant mass of two photon candidates identified in the BGOOD Rugby Ball. Peaks corresponding π^0, η, ω (when two photons from $\omega \rightarrow \pi^0\gamma$ spatially overlap) and η' are labelled. The selection criteria are described in Ref. [5].

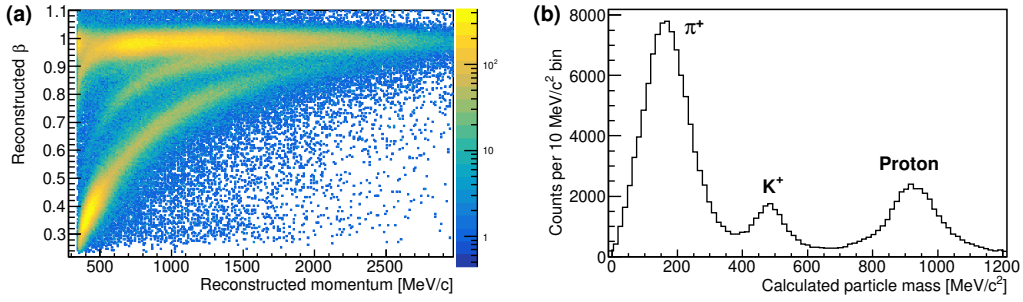

Figure 3: Charged particle identification in the forward spectrometer (only positively charged particles shown). (a) Particle β versus momentum. Characteristic loci corresponding to π^+, K^+ and protons are evident. (b) Calculated particle masses for particles with momentum between 600 and 1000 GeV/c. Figure adapted from Ref. [5].

minimum momentum transfer, t_{min} and $\cos\theta^K_{\text{CM}} = 1$ (Fig. 5, right panel), where it may be regarded as a peak at the $\Sigma(1385)K^+$ threshold. Fitting a Breit-Wigner function to this peak with a polynomial to describe the trend of the data yields a mass and width consistent with the summed $K\Sigma(1385)$ mass and a width of the $\Sigma(1385)$. Numerous model calculations (see for example Ref. [28] and references therein) predict equivalent P_C states in the strangeness sector, where if proven correct, a molecular $\Sigma^0(1385)K^+$ system would be the strange analogue of the $P_C(4382)$ at the $\Sigma^*_C\bar{D}$ threshold.

Preliminary differential cross section data for $K^+\Sigma^-$ photoproduction at $\cos\theta^K_{\text{CM}} > 0.9$ is shown in Fig. 6 (left panel). The BGOOD data is the first data at this forward $\cos\theta^K_{\text{CM}}$ interval from threshold. There appears a structure at the K^+K^-p threshold, which is in agreement with LEPS data that starts at a higher energy. Hadronic molecules with hidden strangeness have been proposed at this threshold which are consistent in mass and width of the observed structure, including bound ϕN systems with a mass of 1950 MeV just below the ϕN threshold [32] and a three-hadron K^+K^-N molecule of $a_0(980)N$ and $f_0(980)N$ components [33]. The importance of accessing forward angles is demonstrated in Fig. 6 (right panel), where the same data is shown differential with respect to the Mandelstam variable, t. The structure at the K^+K^-p threshold resides at a very low t at approximately 0.12 GeV^2. The CLAS data, which is at a more backward $\cos\theta^K_{\text{CM}}$ of 0.8 to 0.9 is at a

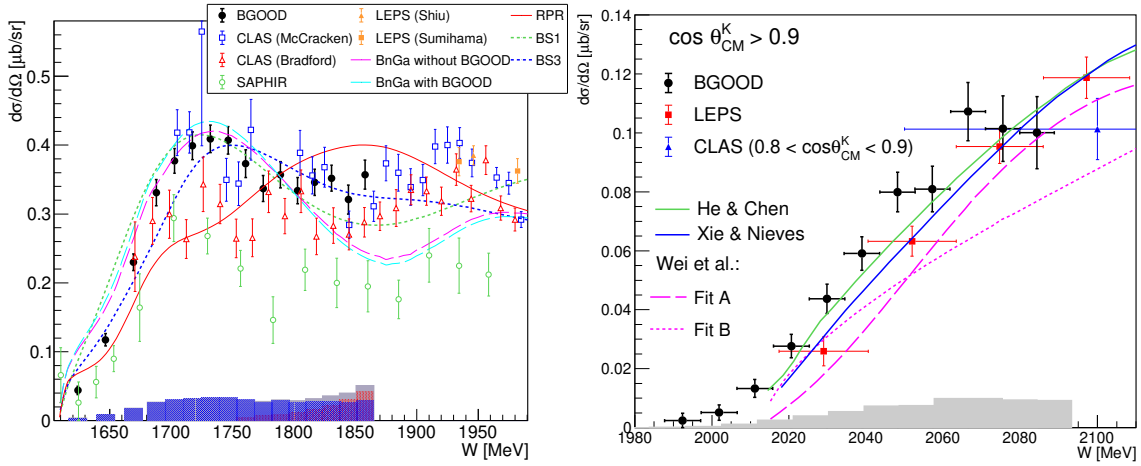

Figure 4: $\gamma p \to K^+\Lambda$ and $\gamma p \to K^+\Lambda(1520)$ differential cross section measurements for $\cos\theta^K_{\rm CM} > 0.90$ (black filled circles). The systematic uncertainties are shown on the abscissa. Previous $K^+\Lambda$ data [15–18] is indicated in the legend (The CLAS data are at the more backward angle of 0.85 $<\cos\theta^K_{\rm CM} < 0.95$). The Regge plus resonant model [19] and isobar models BS1 and BS3 [20, 21] of Skoupil and Bydžovský, and the Bonn-Gatchina PWA [22] solutions with and without the inclusion of the BGOOD data are also shown. For $K^+\Lambda(1520)$, previous LEPS [23] and CLAS data [24] (at the more backward $\cos\theta^K_{\rm CM}$ of 0.8 to 0.9) are shown as filled red squares and filled blue triangles respectively. For all data, vertical bars indicate statistical error and horizontal bars indicate the range of the data point. The results from the effective Lagrangian models of Xie and Nieves [25], He and Chen [26] and Wei *et. al.* [27] are superimposed and labelled inset. Figures from Refs. [10, 12].

much higher t, agreeing with the BGOOD data in this region, suggesting that at forward angles the differential cross section (and the threshold structure) is only dependent on t, and not independently on W and $\cos\theta^K_{\rm CM}$.

2.2 The $\gamma n \to K^0\Sigma^0$ differential cross section over the K^* threshold

The coupled channel model in Ref. [4] purported a dynamically generated $N^*(2030)$ as the origin of a cusp measured in $K^0\Sigma^+$ photoproduction [3], which was also predicted to cause a peak-like structure in $K^0\Sigma^0$. Observing this would therefore provide evidence of a molecular state in the *uds* sector. An example of the differential cross section measured at BGOOD is shown in Fig. 7 [8]. The data are in reasonable agreement with the previous data from the A2 collaboration [37] and in the more forward interval shown, are consistent with the predicted peak from Ref. [4].[1] Further data has now been taken and new analysis techniques to enable a firm interpretation.

2.3 Photoproduction of $K^+\Lambda(1405) \to K^+\pi^0\Sigma^0$

Reference [38] proposes that a triangle singularity contributes to $K^+\Lambda(1405)$ photoproduction, resulting in an enhancement at $W \sim 1900$ MeV. This singularity is driven by the same dynamically generated $N^*(2030)$ predicted in Ref. [4] for $K\Sigma$ photoproduction. This would support the molecular-like structure of the $N^*(2030)$ as it must reside close to the $K^*\Sigma$ threshold and have a strong

[1]The model calculation however is the integrated cross section over all $\cos\theta^K_{\rm CM}$ and set at an arbitrary scale. A differential cross section calculation would be highly desirable for an accurate comparison.

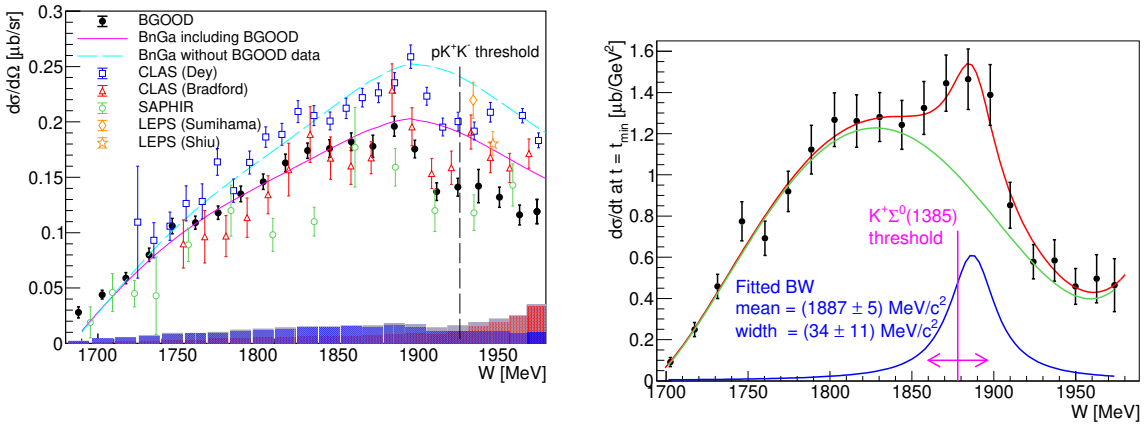

Figure 5: Left: $\gamma p \to K^+\Sigma^0$ differential cross section for $\cos\theta^K_{\rm CM} > 0.90$ (black circles). The systematic uncertainties on the abscissa are in three components described in Ref. [11]. Previous data [16–18, 29, 30] are labelled in the legend. The CLAS data are at the more backward angle of $0.85 < \cos\theta^K_{CM} < 0.95$. The Bonn-Gatchina PWA solutions [31] is also shown with and without the inclusion of the new data. The pK^+K^- threshold is indicated by the dashed black line. Right: $d\sigma/dt$ extrapolated to $t_{\rm min}$ versus W. The sum of a fourth order polynomial and Breit Wigner function is fitted to the data (red line, with constituent components in green and blue respectively). The fitted parameters of the Breit Wigner and the $K^+\Sigma^0(1385)$ threshold are labelled inset.

coupling to the open-strange system. Figure 8 shows the cross section measured at BGOOD [9]. The purple line is the model calculation in Ref. [38] of the triangle singularity being driven by the $N^*(2030)$ resonance, with excellent agreement to the BGOOD data.

Table 1 lists P_C states in the charmed sector and the $\Sigma_c^{(*)}\bar{D}^{(*)}$ thresholds they lie at. This is compared to the equivalent $\Sigma^{(*)}K^{(*)}$ thresholds in the strangeness sector, where there may be mounting evidence of similar molecular-like states. There appears an equivalence between the $P_C(4382)$ at the $\Sigma_c^*\bar{D}$ threshold and a bound $K^+\Sigma^0(1385)$ molecular system, a candidate of which may be seen as a peak in $K^+\Sigma^0$ photoproduction. Moving to the next threshold in energy, there would be an equivalence between the $P_C(4457)$ at the $\Sigma_c\bar{D}^*$ threshold and the proposed $N^*(2030)$ at the Σ^0K^{*+} threshold which may have been observed as a cusp in the $K^0\Sigma^+$ (previous CB/ELSA-TAPS data [41], a peak in $K^0\Sigma^0$ and driving a triangle singularity evident in the $K^+\Lambda(1405)$ cross section.

3. Coherent meson photoproduction off the deuteron at BGOOD

Differential cross sections for the coherent reactions, $\gamma d \to \pi^0\pi^0 d$ [42] (Fig. 9), $\gamma d \to \pi^0\eta d$ [43] (Fig. 10) and $\gamma d \to \pi^0\pi^0\pi^0 d$ (preliminary) [44] have been made with BGOOD where the deuteron is identified in the forward spectrometer (corresponding to $\cos\theta^d_{\rm CM} > 0.8$). All of the differential cross sections are unexpectedly large. The three-momentum transfer to the deuteron ranges between 0.4 and 1.0 GeV/c respectively, which is much higher than the Fermi momentum of the constituent nucleons (typically 80 MeV/c) and therefore what can be transferred to the deuteron for it to remain intact. This is demonstrated in the model calculations in Refs. [45, 46] for $\pi^0\pi^0 d$, which is an order of magnitude smaller at forward angles due to the increasing momentum transfer.

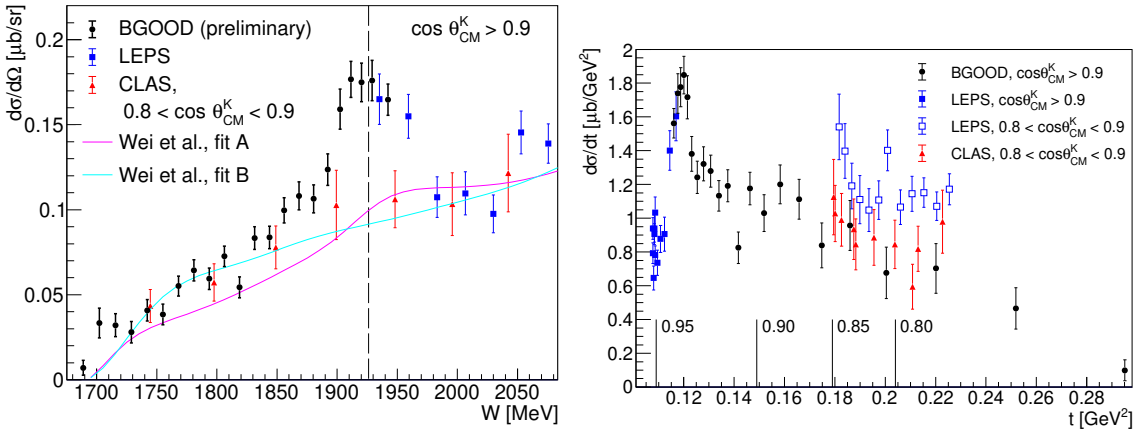

Figure 6: $\gamma p \to K^+\Sigma^-$ differential cross section measurements for $\cos\theta^K_{\rm CM} > 0.9$. Preliminary BGOOD data [13] are shown as black circles and previous data from LEPS [34] and CLAS [35] are blue squares and red triangles respectively (The CLAS data is at the more backward angle of $0.8 < \cos\theta^K_{\rm CM} < 0.9$). The model fits A and B of Wei *et al.* are described in Ref. [36]. The pK^+K^- threshold is indicated by the dashed line. Right panel: $K^+\Sigma^-$ differential cross section data with respect to t. BGOOD (preliminary), LEPS and CLAS data with $\cos\theta^K_{\rm CM}$ intervals are indicated in the legend. The vertical lines on the abscissa indicate the minimum t which can be achieved for the given $\cos\theta^K_{\rm CM}$ over all W.

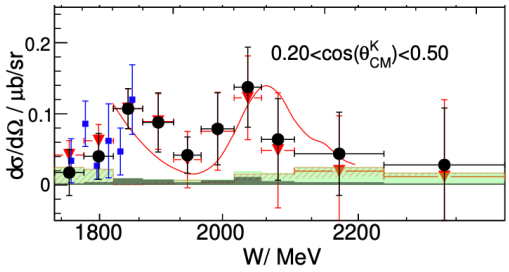

Figure 7: $\gamma n \to K^0\Sigma^0$ differential cross section for $0.2 < \cos\theta^K_{\rm CM} < 0.5$, employing two different fitting methods for yield extraction (red triangles and black circles). The blue squares are data from the A2 Collaboration [37]. The predicted total cross section from Ref. [4] is shown as the red line at an arbitrary scale. Figure adapted from Ref. [8].

The origin of the unexpectedly large cross sections is not yet clear. One suggestion could be the formation of intermediate dibaryons, for example the $d^*(2380)$ [50, 51]. Alternatively, there may be large contributions from final state interactions, for example the diagrams shown in Fig. 10 (right panel). To test this hypothesis, a toy model of the two diagrams was made, assuming on-shell kinematics, which gives an excellent description of the data. Detailed quantitative model calculations, for example Ref. [46] however suggest that final state interactions contribute only a few percent of the measured cross section (black line in Fig. 10).

4. The INSIGHT experiment at ELSA

The new INSIGHT experiment (Fig. 11), is an important upgrade for both the BGOOD and Crystal Barrel photoproduction experiments at ELSA. INSIGHT will feature a unique combination

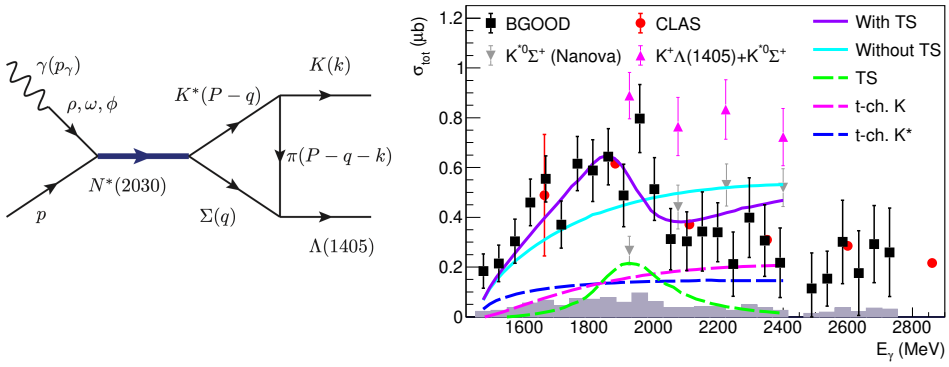

Figure 8: Left: The proposed triangle singularity driving $K^+\Lambda(1405)$ photoproduction. Right: The integrated cross section for $\gamma p \to K^+\Lambda(1405) \to K^+\pi^0\Sigma^0$. The purple (cyan) line is the model of Wang *et al.* [38] with (without) the triangle singularity, with t-channel exchange contributions labelled in the legend. The $K^{*0}\Sigma^+$ data from CBELSA/TAPS [39] are the grey triangles and the sum of the $K^{*0}\Sigma^+$ and the BGOOD $K^+\Lambda(1405)$ data are the magenta triangles. Figures from Refs. [38] and [9].

Charm sector		Strange sector	
Threshold	State	Threshold	Evidence
$\Sigma_c\bar{D}$	$P_C(4312)$	Σ^0K^+ at 1687 MeV	$N(1535)$
$\Sigma_c^*\bar{D}$	$P_C(4382)$	$\Sigma^0(1385)K^+$ at 1879 MeV	Peak in $K^+\Sigma^0$ at t_{min} (BGOOD [11])
-	No equivalent	K^+K^-N at 1926 MeV	Structure in $K^+\Sigma^-$ at low t (BGOOD [13])
$\Sigma_c\bar{D}^*$	$P_C(4457)$	Σ^0K^{*+} at 2085 MeV	Cusp in $K^0\Sigma^+$ (CB/ELSA-TAPS [41]), (Tentative) peak in $K^0\Sigma^0$ (BGOOD [8]), Triangle singularity in $K^+\Lambda(1405)$ (BGOOD [9])

Table 1: Comparison between P_C states and their proximity to thresholds to $K\Sigma$ thresholds and evidence of molecular states. The $P_C(4382)$ is a suggestion from Du *et al.* [40].

of an almost complete angular coverage for high-resolution photon measurements, charged-particle detection and the ability to perform measurements using a polarized beam and a polarized target. For high resolution photon measurements the detector will reuse the main calorimeter of the CBELSA/TAPS experiment and in forward direction the PANDA Forward endcap consisting of 3856 $PbWO_4$ crystals. A new pixel vertex detector for charged particles installed in the space between the target and the calorimeter will measure the trajectories of charged particles with high precision and ensure good vertex resolution. A new forward spectrometer, consisting of several planes of

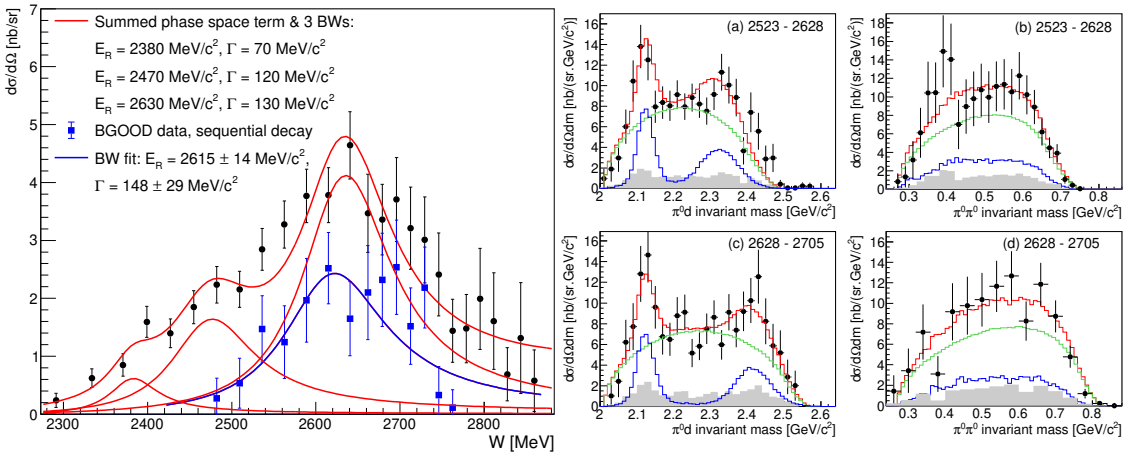

Figure 9: Left panel: $\gamma d \rightarrow \pi^0\pi^0 d$ differential cross section for $\cos\theta^d_{\mathrm{CM}} > 0.8$, where the error bars are the statistical and systematic uncertainties summed quadratically. A fit including three Breit-Wigner functions (BW) representing proposed isoscalar dibaryons is shown as the red lines, with the fixed masses and widths labelled inset. The blue square data points is the differential cross section for the proposed isovector dibaryon which was determined from the $\pi^0 d$ invariant mass distributions (examples shown in the right panel). The fitted distributions to the $\pi^0 d$ invariant masses (red line) is comprised of phase space (green line) and proposed sequential dibaryon decay (blue line) contributions. Figures from Refs. [42].

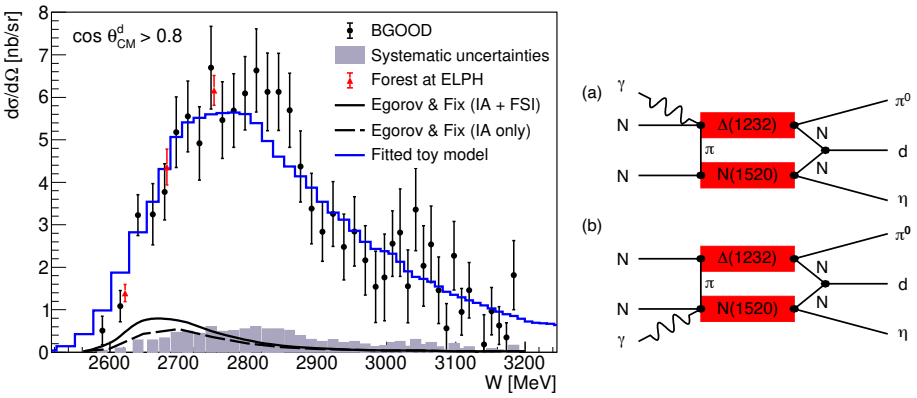

Figure 10: Left: The $\gamma d \rightarrow \eta\pi^0 d$ differential cross section for $\cos\theta^d_{\mathrm{CM}} > 0.8$ (black circles, with systematic uncertainties indicated as grey bars on the abscissa. Superimposed are data from the Forest detector at the ELPH facility [47] and the phenomenological models of Egorov and Fix [48, 49]. solid and dashed lines are with or without the inclusion of final state interactions respectively. Right: Two proposed mechanisms contributing to the cross section. Figures from Ref. [43].

high-resolution tracking detectors up- and downstream of a new dipole magnet and a forward time-of-flight wall will provide charged particle identification and momentum reconstruction. INSIGHT will enable unique possibilities in understanding strange and non-strange baryon resonance spectra and states including their properties. In addition, it will build upon the research of unconventional baryon structure pursued with BGOOD, addressing the issue of whether exotic states such as pentaquarks observed in the charmed sector also exist in the strange sector.

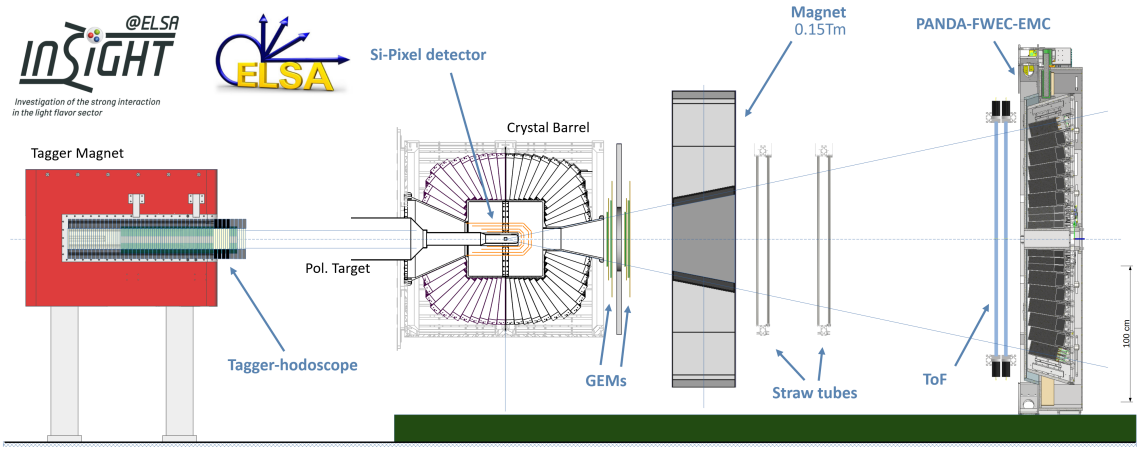

Figure 11: The new INSIGHT experiment at the ELSA facility at the University of Bonn.

Acknowledgements

This work is supported by the Deutsche Forschungsgemeinschaft Project Numbers 388979758 and 405882627, the Third Scientific Committee of the INFN and has received funding from the European Union's Horizon 2020 research and innovation programme under grant agreement STRONG–2020 No. 824093.

References

[1] R. Aaij, et al., Phys. Rev. Lett. 115 (2015) 072001.

[2] R. Aaij, et al., Phys. Rev. Lett. 122 (2019) 222001.

[3] R. Ewald, et al., Phys. Lett. B 713 (2012) 180.

[4] A. Ramos, E. Oset, Phys. Lett. B 727 (2013) 287.

[5] S. Alef, et al., Eur. Phys. J. A 56 (2020) 104.

[6] W. Hillert, Eur. Phys. J. A 28 (2006) 139 (2006).

[7] W. Hillert, et al., EPJ Web Conf. 134 (2017) 05002.

[8] K. Kohl, T. C. Jude, et al., Eur. Phys. J. A 59 (2023) 254.

[9] G. Scheluchin, T. C. Jude, et al., Phys. Lett. B 833 (2022) 137375.

[10] S. Alef, et al., Eur. Phys. J. A 57 (2021) 80.

[11] T. C. Jude, et al., Phys. Lett. B 820 (2021) 136559.

[12] E. O. Rosanowski, T. C. Jude, et al., Eur. Phys. J. A 61 (2025) 147.

[13] J. Groß, Ph.D. thesis, The University of Bonn (In preparation).

[14] M. Jena, Masters thesis, The University of Bonn (2024).

[15] M. E. McCracken, et al., Phys. Rev. C 81 (2010) 025201.

[16] R. Bradford, et al., Phys. Rev. C 81 (2006) 035202.

[17] M. Sumihama, et al., Phys. Rev. C 73 (2006) 035214.

[18] S. H. Shiu, H. Kohri, et al., Phys. Rev. C 97 (2018) 015208.

[19] P. Bydžovský, D. Skoupil, Phys. Rev. C 100 (2019) 035202.

[20] D. Skoupil, P. Bydžovský, Phys. Rev. C 93 (2016) 025204.

[21] D. Skoupil, P. Bydžovský, Phys. Rev. C 97 (2018) 025202.

[22] Bonn-gatchina partial wave analysis, URL https://pwa.hiskp.uni-bonn.de

[23] H. Kohri, et al., Phys. Rev. Lett. 104 (2010) 172001.

[24] K. Moriya, et al., Phys. Rev. C 88 (2013) 045201.

[25] J. J. Xie, J. Nieves, Phys. Rev. C 82 (2010) 045205.

[26] J. He, X.-R. Chen, Phys. Rev. C 86 (2012) 035204.

[27] N. C. Wei, Y. Zhang, F. Huang, D. M. Li, Phys. Rev. D 103 (2021) 034007.

[28] H. Huang, X. Zhu, J. Ping, Phys. Rev. D 97 (2018) 094019.

[29] B. Dey, et al., Phys. Rev. C 82 (2010) 025202.

[30] K. Glander, et al., Eur. Phys. J. A 19 (2004) 251.

[31] A. V. Anisovich, et al., Eur. Phys. J. A 50 (2014) 129.

[32] H. Gao, H. Huang, T. Liu, J. Ping, F. Wang, Z. Zhao, Phys. Rev. C 95 (2017) 055202 (2017).

[33] A. Martínez Torres, K. P. Khemchandani, U.-G. Meißner, E. Oset, Eur. Phys. J. A 41 (2009) 361.

[34] H. Kohri, et al., Phys. Rev. Lett. 97 (2006) 082003.

[35] S. A. Pereira, et al., Phys. Lett. B 688 (2010) 289.

[36] N.-C. Wei, A.-C. Wang, F. Huang, Phys. Rev. D 107 (2023) 114018.

[37] C. S. Akondi, K. Bantawa, et al., Eur. Phys. J. A 55 (2019) 202.

[38] E. Wang, et al., Phys. Rev. C 95 (2017) 015205.

[39] M. Nanova, et al., Eur. Phys. J. A 35 (2008) 333.

[40] M.-L. Du, V. Baru, F.-K. Guo, C. Hanhart, U.-G. Meißner, J. A. Oller, Q. Wang, Phys. Rev. Lett. 124 (2020) 072001.

[41] R. Ewald et al., Phys. Lett. B 713 (2012) 180.

[42] T. C. Jude, et al., Phys. Lett. B 832 (2022) 137277.

[43] A. J. C. Figueiredo, T. C. Jude, et al., arXiv:2405.09392 (2024).

[44] R. Volk, Master's thesis, The University of Bonn (2024).

[45] A. Fix, H. Arenhövel, Eur. Phys. J. A 25 (2005) 115.

[46] M. Egorov, A. Fix, Nucl. Phys. A 933 (2015) 104.

[47] T. Ishikawa, et al., Phys. Rev. C 105 (2022) 045201.

[48] M. Egorov, A. Fix, Phys Rev. C 88 (2013) 054611.

[49] A. Fix, private communication (2024).

[50] P. Adlarson, et al., Phys. Rev. Lett. 106 (2011) 242302.

[51] M. Bashkanov, et al., Phys. Rev. Lett. 102 (2009) 052301.